Inorg. Chem. **2006**, *45*, 7535–7543

Forum

Solution-Grown Zinc Oxide Nanowires

Lori E. Greene, Benjamin D. Yuhas, Matt Law, David Zitoun, and Peidong Yang*

Department of Chemistry, University of California, Berkeley, California 94720, and Materials Sciences Division, Lawrence Berkeley National Laboratory, Berkeley, California 94720

Received February 3, 2006

We review two strategies for growing ZnO nanowires from zinc salts in aqueous and organic solvents. Wire arrays with diameters in the nanoscale regime can be grown in an aqueous solution of zinc nitrate and hexamethylenetetramine. With the addition of poly(ethylenimine), the lengths of the wires have been increased to 25 μm with aspect ratios over 125. Additionally, these arrays were made vertical by nucleating the wires from oriented ZnO nanocrystals. ZnO nanowire bundles have been produced by decomposing zinc acetate in trioctylamine. By the addition of a metal salt to the solution, the ZnO wires can be doped with a range of transition metals. Specifically, ZnO nanowires were homogeneously doped with cobalt and showed a marked deviation from paramagnetic behavior. We conclude by highlighting the use of these solution-grown nanowire arrays in dye-sensitized solar cells. The nanowire cells showed an improvement in the charge collection efficiency over traditional nanoparticle cells.

Introduction

Zinc oxide (ZnO) is a commercially important material used in paints, protective coatings for metals, rubber processing, and sunscreens because it is abundant and nontoxic. In the past decade, ZnO thin films and nanostructures have become promising materials for emerging electronic applications. ZnO is a wide band gap (3.37 eV) semiconductor with a large exciton binding energy (60 meV) and an exciton Bohr radius in the range of 1.4−3.5 nm.[1] ZnO nanowires are important because of their unique structural one-dimensionality and possible quantum confinement effects in two dimensions.[2] They can possess novel electronic and optical properties with uses as room-temperature ultraviolet (UV) lasers,[3] field-effect transistors,[4] photodetectors,[5] gas sensors,[6] and solar cells.[7] In addition, magnetic and electrical properties can be modified by intentionally introducing impurities into the lattice. Transition-metal-doped ZnO wires are a model material system for dilute magnetic semiconductors (DMSs).[8]

One-dimensional ZnO nanostuctures are easily synthesized owing to facile growth along the *c* axis of the wurtzite crystal, which has a hexagonal unit cell with six nonpolar $\{10\bar{1}0\}$ prismatic faces capped by polar oxygen $(000\bar{1})$ and zinc (0001) basal planes. The polar faces are electrostatically unstable Tasker type III surfaces,[9] making the {0001} planes have the highest energy of the low-index surfaces. This suggests a growth habit where the *c* axis is the fastest-growing direction. The growth rates of various surfaces can also be kinetically controlled, especially in the case of solution-phase syntheses at moderate temperatures. For example, the growth of certain surfaces can be impeded by using additives that preferentially adsorb to specific crystal faces.[2]

ZnO nanowires are most commonly synthesized by gas-phase approaches such as metal−organic chemical vapor

* To whom correspondence should be addressed. E-mail: p_yang@uclink.berkeley.edu.

(1) Reynolds, D. C.; Look, D. C.; Jogai, B.; Litton, C. W.; Collins, T. C.; Harsch, W.; Cantwell, G. *Phys. Rev. B* **1998**, *57*, 12151−12155.
(2) Law, M.; Goldberger, J.; Yang, P. D. *Annu. Rev. Mater. Res.* **2004**, *34*, 83−122.
(3) Huang, M. H.; Mao, S.; Feick, H.; Yan, H. Q.; Wu, Y. Y.; Kind, H.; Weber, E.; Russo, R.; Yang, P. D. *Science* **2001**, *292*, 1897−1899.
(4) Goldberger, J.; Sirbuly, D. J.; Law, M.; Yang, P. *J. Phys. Chem. B* **2005**, *109*, 9−14.
(5) Kind, H.; Yan, H. Q.; Messer, B.; Law, M.; Yang, P. D. *Adv. Mater.* **2002**, *14*, 158−160.
(6) Wan, Q.; Li, Q. H.; Chen, Y. J.; Wang, T. H.; He, X. L.; Li, J. P.; Lin, C. L. *Appl. Phys. Lett.* **2004**, *84*, 3654−3656.
(7) Law, M.; Greene, L. E.; Johnson, J. C.; Saykally, R.; Yang, P. D. *Nat. Mater.* **2005**, *4*, 455−459.
(8) Norberg, N. S.; Kittilstved, K. R.; Amonette, J. E.; Kukkadapu, R. K.; Schwartz, D. A.; Gamelin, D. R. *J. Am. Chem. Soc.* **2004**, *126*, 9387−9398.
(9) Tasker, P. W. *J. Phys. C: Solid State Phys.* **1979**, *12*, 4977−4984.

10.1021/ic0601900 CCC: $33.50
Published on Web 09/11/2006

deposition,[10,11] chemical vapor transport,[12,13] and pulsed laser deposition.[14] These methods can produce high-quality, single-crystalline wires with lengths of several microns. However, these processes require elevated temperatures of 450−900 °C and often face other limitations in terms of sample uniformity, substrate choice, and low product yield. In contrast, solution approaches are appealing because of the low growth temperatures (<350 °C), potential for scaling up, and straightforward methods of producing high-density arrays (nanowire number density $>10^{10}$ cm^{-2}).[15]

In this Article, we focus on the synthesis of ZnO nanowires from zinc salts in solution. We concentrate on the following two methods: the hydrolysis of zinc nitrate [$Zn(NO_3)_2 \cdot 6H_2O$] in water with the addition of hexamethylenetetramine (HMTA)[15] and the decomposition of zinc acetate [$Zn(CH_3CO_2)_2$] in trioctylamine.[16] The quality of the resulting wires has been characterized by scanning electron microscopy (SEM), transmission electron microscopy (TEM), and photoluminescence (PL). The shape dependence of the products on pH, solvent, and different additives is reviewed to elucidate possible growth mechanisms. Wires grown using zinc acetate in trioctylamine have been doped with transition metals (cobalt, manganese, iron, and copper) with an emphasis on cobalt-doped wires. Cobalt-doped wires have been characterized by SEM, TEM, PL, X-ray diffraction (XRD), and electron paramagnetic resonance (EPR) to verify doping uniformity and to investigate their magnetic properties. Additionally, we will discuss a method of producing vertical nanowire arrays from substrates coated with ZnO seeds that are aligned with their *c* axes normal to the surface.[17] Decomposing a thin layer of zinc acetate on a surface forms these textured seeds. We conclude with results on the use of nanowire arrays as the photoanode in dye-sensitized solar cells (DSCs).[7] Comparisons with conventional nanoparticle cells show that the nanowire geometry is a superior current collector.

Synthesis of One-Dimensional ZnO Nanostructures in Solution

Hydrolysis of Zinc Salts in Water. In aqueous solution, zinc(II) is solvated by water, giving rise to aquo ions. In dilute solutions, zinc(II) can exist as several monomeric hydroxyl species.[18] These species include $ZnOH^+$(aq), $Zn(OH)_2$(aq), $Zn(OH)_2$(s), $Zn(OH)_3^-$(aq), and $Zn(OH)_4^{2-}$(aq). At a given zinc(II) concentration, the stability of these complexes is dependent on the pH and temperature of the solution.[19] Solid ZnO nuclei are formed by the dehydration of these hydroxyl species. The ZnO crystal can continue to grow by the condensation of the surface hydroxyl groups with the zinc−hydroxyl complexes.[19]

The hydrolysis and condensation reactions of zinc salts result in one-dimensional ZnO crystals under a wide variety of conditions. In general, rod/wire growth is possible in slightly acidic to basic conditions ($5 < pH < 12$) at temperatures from 50 to 200 °C. Wires are formed at pH > 9 even in the absence of additives.[20−22] Basic conditions are crucial because divalent metal ions do not readily hydrolyze in acidic media.[23] For growth at pH < 9, an additive such as HMTA or dimethylamineborane (DMBA) must be used to promote one-dimensional ZnO precipitation. It has been suggested[19] that these additives function, in part, by decomposing during the reaction and increasing the pH to above ~9 at the crystal surface.

The crystal morphology can be controlled by various species in the solution, which act as promoters or inhibitors for nucleation and growth. These species can include the zinc counterion, additives such as amines, and acids and bases. In general, additives such as DMBA[24,25] and sodium citrate[26] form platelets, while rods (aspect ratio < 10) and wires (aspect ratio > 10) form in the presence of amines such as HMTA,[15,23,27−30] ethylenediamine,[31,32] triethanolamine,[32] and diethylenetriamine.[15,33] The effect of the counterion was examined by Govender et al.[18] for solutions containing HMTA. Solutions containing acetate, formate, or chloride mainly formed rods, nitrate or perchlorate produced wires, and sulfate yielded flat hexagonal platelets. Although pH may play an important role in this case, these results show that the species in solution can have a strong effect on the resulting morphology.

The most successful and well-studied condensation reaction for ZnO wire growth is the hydrolysis of zinc nitrate in water in the presence of HMTA. The zinc nitrate and HMTA

(10) Park, W. I.; Yi, G. C.; Kim, M. Y.; Pennycook, S. J. *Adv. Mater.* **2002**, *14*, 1841−1843.
(11) Wu, J. J.; Liu, S. C. *Adv. Mater.* **2002**, *14*, 215−218.
(12) Yang, P. D.; Yan, H. Q.; Mao, S.; Russo, R.; Johnson, J.; Saykally, R.; Morris, N.; Pham, J.; He, R. R.; Choi, H. J. *Adv. Funct. Mater.* **2002**, *12*, 323−331.
(13) Yao, B. D.; Chan, Y. F.; Wang, N. *Appl. Phys. Lett.* **2002**, *81*, 757−759.
(14) Sun, Y.; Fuge, G. M.; Ashfold, M. N. R. *Chem. Phys. Lett.* **2004**, *396*, 21−26.
(15) Greene, L. E.; Law, M.; Goldberger, J.; Kim, F.; Johnson, J. C.; Zhang, Y. F.; Saykally, R. J.; Yang, P. D. *Angew. Chem., Int. Ed.* **2003**, *42*, 3031−3034.
(16) Yuhas, B. D.; Zitoun, D. O.; Pauzauskie, P. J.; He, R.; Yang, P. *Angew. Chem., Int. Ed.* **2006**, *45*, 420−423.
(17) Greene, L. E.; Law, M.; Tan, D. H.; Montano, M.; Goldberger, J.; Somorjai, G.; Yang, P. D. *Nano Lett.* **2005**, *5*, 1231−1236.
(18) Govender, K.; Boyle, D. S.; Kenway, P. B.; O'Brien, P. *J. Mater. Chem.* **2004**, *14*, 2575−2591.
(19) Yamabi, S.; Imai, H. *J. Mater. Chem.* **2002**, *12*, 3773−3778.
(20) Chittofrati, A.; Matijevic, E. *Colloids Surf.* **1990**, *48*, 65−78.
(21) McBride, R. A.; Kelly, J. M.; McCormack, D. E. *J. Mater. Chem.* **2003**, *13*, 1196−1201.
(22) Peterson, R. B.; Fields, C. L.; Gregg, B. A. *Langmuir* **2004**, *20*, 5114−5118.
(23) Verges, M. A.; Mifsud, A.; Serna, C. J. *J. Chem. Soc., Faraday Trans.* **1990**, *86*, 959−963.
(24) Izaki, M.; Omi, T. *J. Electrochem. Soc.* **1997**, *144*, L3−L5.
(25) Cao, B. Q.; Cai, W. P.; Duan, G. T.; Li, Y.; Zhao, Q.; Yu, D. P. *Nanotechnology* **2005**, *16*, 2567−2574.
(26) Tian, Z. R. R.; Voigt, J. A.; Liu, J.; McKenzie, B.; McDermott, M. J. *J. Am. Chem. Soc.* **2002**, *124*, 12954−12955.
(27) Chou, K. S.; Chen, W. H.; Huang, C. S. *J. Chin. Inst. Chem. Eng.* **1990**, *21*, 327−334.
(28) Music, S.; Popovic, S.; Maljkovic, M.; Dragcevic, E. *J. Alloys Compd.* **2002**, *347*, 324−332.
(29) Vayssieres, L. *Adv. Mater.* **2003**, *15*, 464−466.
(30) Vayssieres, L.; Keis, K.; Lindquist, S. E.; Hagfeldt, A. *J. Phys. Chem. B* **2001**, *105*, 3350−3352.
(31) Obrien, P.; Saeed, T.; Knowles, J. *J. Mater. Chem.* **1996**, *6*, 1135−1139.
(32) Trindade, T.; Dejesus, J. D. P.; Obrien, P. *J. Mater. Chem.* **1994**, *4*, 1611−1617.
(33) Zhang, H.; Yang, D. R.; Ma, X. Y.; Que, D. L. *J. Phys. Chem. B* **2005**, *109*, 17055−17059.

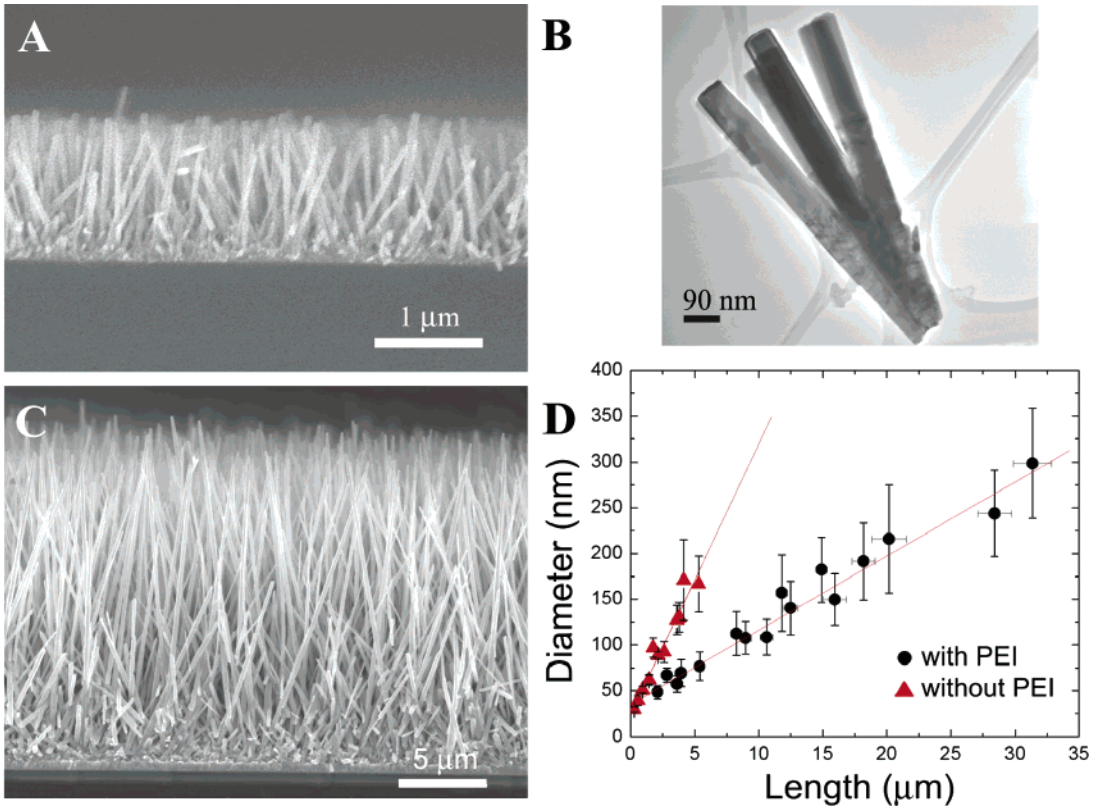

Figure 1. Analysis of ZnO nanowire arrays grown in water with zinc nitrate and HMTA at 90 °C. (A) Cross-sectional SEM image of an array grown for 1.5 h on a silicon wafer. (B) TEM image of a cluster of ZnO nanowires removed from an array grown for 1.5 h on a silicon wafer. (C) SEM cross section of a cleaved nanowire array grown with the addition of PEI on a fluorine-doped tin oxide substrate. (D) Wire diameter versus length with (circles) and without (triangles) PEI added to the growth bath. Lines are least-squares fits to the data, and error bars represent 1 standard deviation. Reprinted with permission from ref 15. Copyright 2003 Wiley-VCH. Reprinted with permission from ref 7. Copyright 2005 Nature.

concentrations should, in general, be less than 0.1 M, with $5 < \text{pH} < 8$ and the temperature >80 °C.[23,27,34] This synthesis produces wires and rods with diameters on the micron scale. Growth from a substrate coated in a thin layer of ZnO nanoparticles decreases the diameter to below 200 nm. Several studies[29,35] have shown that smaller seeds yield thinner wires. We have shown that ZnO nanowire arrays can be grown using a seeded substrate suspended in an open crystallizing dish filled with an aqueous solution of zinc nitrate hydrate (0.025 M) and HMTA (0.025 M) at 90 °C.[15] ZnO seeds (diameter = 5 nm) were dip-coated several times on a substrate. Figure 1A is a SEM image of a typical 1.5-h synthesis; wire diameters range between 40 and 80 nm, lengths are 1.5−2 μm, and the average aspect ratio is 30. TEM characterization of individual nanowires reveals that they are single-crystalline and grow in the [0001] direction (Figure 1B). By decreasing the concentration of the reactants, the diameter of these wires can be further reduced,[29,36] but a reduction in length is also seen. To obtain long wires, the samples must be repeatedly introduced into fresh solution baths every several hours. Eventually, the diameters will continue to increase until the wires fuse together to form a thin film.

The role of HMTA is still under debate. HMTA is a nonionic cyclic tertiary amine that can act as a Lewis base to metal ions and has been shown to be a bidentate ligand capable of bridging two zinc(II) ions in solution.[27,37] HMTA is also known to hydrolyze, producing formaldehyde and ammonia in the pH and temperature range of the ZnO nanowire reaction.[38] In this case, HMTA acts as a pH buffer by slowly decomposing to provide a gradual and controlled supply of ammonia, which can form ammonium hydroxide as well as complex zinc(II) to form $Zn(NH_3)_4^{2+}$.[18,39] Because dehydration of the zinc hydroxide intermediates controls the growth of ZnO, the slow release of hydroxide may have a profound effect on the kinetics of the reaction. Additionally, ligands such as HMTA and ammonia can kinetically control species in solution by coordinating to zinc(II) and keeping the free zinc ion concentration low. HMTA and ammonia can also coordinate to the ZnO crystal, hindering the growth of certain surfaces. With additional systematic studies, one or all of these mechanisms may be found to be responsible for the HMTA shape control.

The zinc nitrate and HMTA synthesis is an effective way to achieve high-quality ZnO nanowire arrays but lacks the ability to produce wires with high aspect ratios (>50). High aspect ratio wires are possible by introducing an additional molecule that inhibits radial growth but allows axial growth of the nascent nanowire. Both amines and diblock copoly-

(34) Sakka, Y.; Halada, K.; Ozawa, E. *Ceram. Trans.* **1988**, *1*, 31−38.
(35) Guo, M.; Diao, P.; Cai, S. M. *J. Solid State Chem.* **2005**, *178*, 1864−1873.
(36) Hung, C. H.; Whang, W. T. *Mater. Chem. Phys.* **2003**, *82*, 705−710.
(37) Ahuja, I. S.; Yadava, C. L.; Singh, R. *J. Mol. Struct.* **1982**, *81*, 229−234.
(38) Strom, J. G.; Jun, H. W. *J. Pharm. Sci.* **1980**, *69*, 1261−1263.
(39) Wang, Z.; Qian, X. F.; Yin, J.; Zhu, Z. K. *Langmuir* **2004**, *20*, 3441−3448.

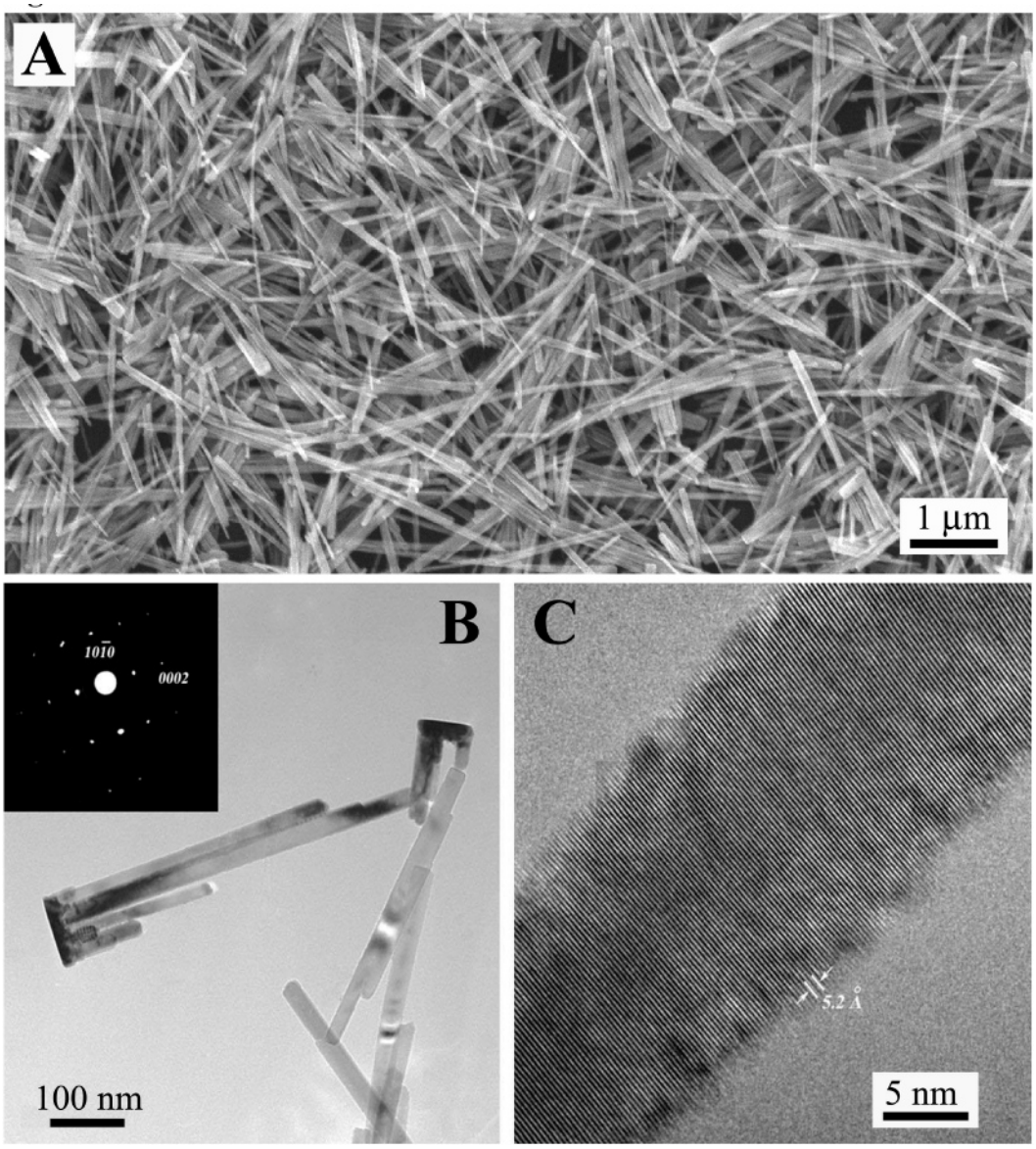

Figure 2. Characterization of ZnO nanowires synthesized by decomposing zinc acetate at ~300 °C in trioctylamine. (A) SEM micrograph of wires grown for 1 h. (B) TEM image of several nanostructures showing the parallel nanowires and nanorods. The inset is a diffraction pattern taken from a single-crystalline ensemble; both the base and wires grow along the [0001] direction. (C) High-resolution TEM image of a single nanowire (16 nm in diameter).

mers[40,41] have been shown to do this. By the addition of low-molecular-weight poly(ethylenimine) (PEI) to the solution, we have shown that long nanowires are formed with aspect ratios greater than 125 (Figure 1C).[7] Figure 1D shows the marked effect of adding PEI to the nanowire growth bath. Wire diameters of ~20−300 nm, lengths of ~50 nm to 25 μm, and aspect ratios of 5−150 can be made by adjusting the reactant concentration, the temperature, and the growth time. On the other hand, ZnO platelets are formed if a low concentration of sodium citrate is added instead of PEI.[26] PEI and citrate could preferentially adsorb to different crystal faces, modifying the surface free energy and growth rate. These effects demonstrate the flexibility of this reaction to create ZnO nanostructures with a variety of shapes and sizes.

Decomposition of Zinc Salts in a Nonaqueous Solvent. In addition to many reports of ZnO nanowire syntheses in aqueous solutions, there are a few methods for obtaining ZnO nanowires in organic solvents. Recently, we reported the formation of ZnO nanowires by decomposing zinc acetate (2.66 mmol) at 300 °C in trioctylamine, a coordinating tertiary amine.[16] A similar method has been used to form ZnO nanorods and nanocrystals of CuO and MnO.[42−44] For undoped ZnO, a small amount of oleic acid (0.15 mol equiv to Zn^{2+}) is added to aid the reaction. A typical synthesis yields nanowires with diameters of 30 ± 5 nm and lengths that range from 0.5 to 5 μm (Figure 2). Interestingly, these nanowires grow from a thin platelet base and are parallel to each other to form a bundle. High-resolution TEM charac-

(40) Oner, M.; Norwig, J.; Meyer, W. H.; Wegner, G. *Chem. Mater.* **1998**, *10*, 460−463.
(41) Taubert, A.; Kubel, C.; Martin, D. C. *J. Phys. Chem. B* **2003**, *107*, 2660−2666.
(42) Yin, M.; Gu, Y.; Kuskovsky, I. L.; Andelman, T.; Zhu, Y.; Neumark, G. F.; O'Brien, S. *J. Am. Chem. Soc.* **2004**, *126*, 6206−6207.
(43) Yin, M.; O'Brien, S. *J. Am. Chem. Soc.* **2003**, *125*, 10180−10181.
(44) Yin, M.; Wu, C. K.; Lou, Y. B.; Burda, C.; Koberstein, J. T.; Zhu, Y. M.; O'Brien, S. *J. Am. Chem. Soc.* **2005**, *127*, 9506−9511.

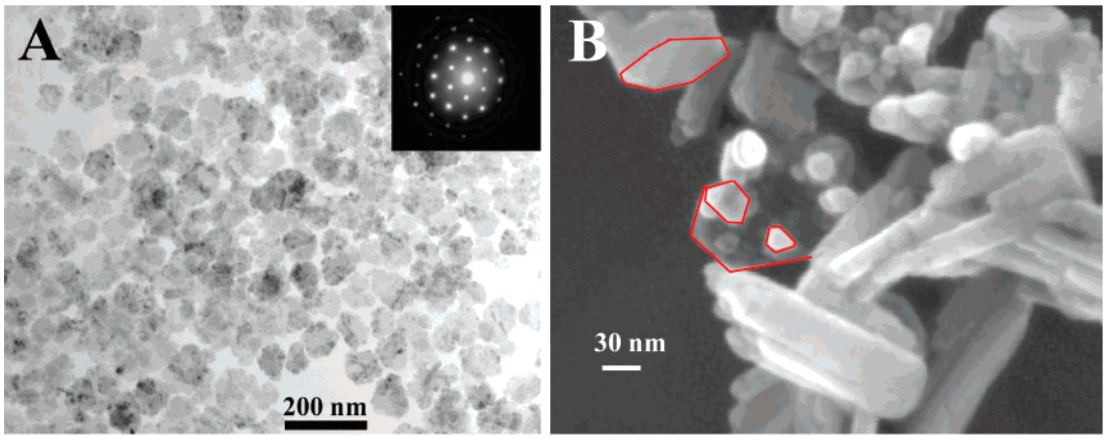

Figure 3. Analysis of ZnO growth steps. (A) TEM image of ZnO platelike nanocrystals. The inset is a diffraction pattern of an individual nanoplate. (B) SEM image of wire bundles where the reaction was stopped at an intermediate growth stage. The hexagonal cross sections are highlighted.

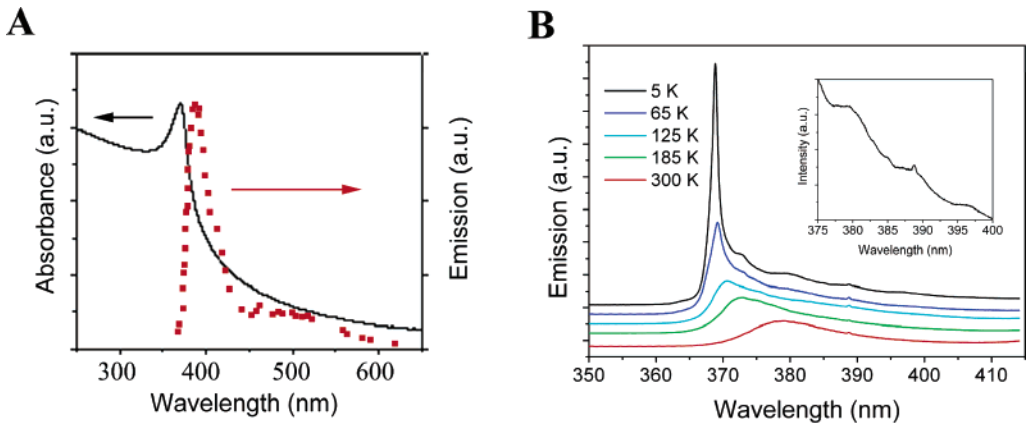

Figure 4. Optical characterization of ZnO nanowires. (A) Absorption and emission spectra of a ZnO nanowire solution. (B) Temperature-dependent PL spectra of a single wire deposited on a silica wafer showing a 90-meV blue shift from room temperature to 5 K. Inset: Detail of the 5 K spectrum.

terization and electron diffraction of individual nanostructures indicate that both the base and wires are single-crystalline and the wires grow along the [0001] direction (Figure 2B,C). This unique parallel growth of densely packed nanowires from a thin single-crystalline base can be explained in two different ways. (i) Individual nanowires self-assemble in solution and form bundles, or (ii) the thin platelike base forms first and acts as a seed for epitaxial nanowire growth. The reaction was stopped at an early growth to further examine the mechanism. SEM images show nanorods growing from flat, hexagonal crystallites while maintaining the same orientation and symmetry (Figure 3). This suggests an epitaxial growth mechanism (growth mechanism ii), where a two-step growth process leads to a single-crystalline bundle.

The high optical quality of the as-grown wires was verified with absorption and PL studies (Figure 4). The absorption spectrum of a 2-propanol solution of nanowires shows a sharp peak at 3.35 eV corresponding to the band gap of bulk ZnO. The emission profile shows a marked band edge at 3.2 eV. It should be noted that the emission does not exhibit any solvent quenching effects and the band-gap emission is remarkably intense for a solution-phase sample.[45] Absorption and PL were acquired with a continuous-wave laser source (HeCd, 325 nm) on individual wires cast onto a clean silicon substrate. Low-temperature PL reveals a blue shift of 90 meV in the band-edge emission from room temperature to 5 K (Figure 4B). At 5 K, a well-resolved donor-bound exciton peak at 368.87 nm (3.361 eV) and corresponding first-, second-, and third-order phonon replicas at 379.56 nm (3.266 eV), 389.23 nm (3.185 eV), and 397.04 nm (3.123 eV) are visible. The shoulder at 364.1 nm (3.404 eV) is attributed to the free exciton transition. The peak centered at 372.8 nm (3.326 eV) is assigned to a two-electron (2e) transition that has been shown to emerge with donor-bound excitons.[1,46]

Trioctylamine acts as a coordinating solvent with one-dimensional growth enabled by the presence of an amine moiety, similar to the effect of PEI in the aqueous synthesis. Interestingly, a recent study by Andelman et al.[47] varies the shape of ZnO by thermally decomposing zinc acetate in different coordinating organic solvents. The morphology of ZnO was highly dependent on the solvent, with trioctylamine yielding nanorods, 1-hexadecanol yielding nanotriangles, and 1-octadecene yielding spherical nanoparticles. Trioctylamine is believed to be a strong coordinating solvent and encourages growth along one direction, while 1-octadecene is not a coordinating solvent, with the resulting spherical particle having no crystal plane preferentially favored as the growth direction.

(45) van Dijken, A.; Meulenkamp, E. A.; Vanmaekelbergh, D.; Meijerink, A. *J. Phys. Chem. B* **2000**, *104*, 4355−4360.

(46) Dean, P. J.; Cuthbert, J. D.; Thomas, D. G.; Lynch, R. T. *Phys. Rev. Lett.* **1967**, *18*, 122.

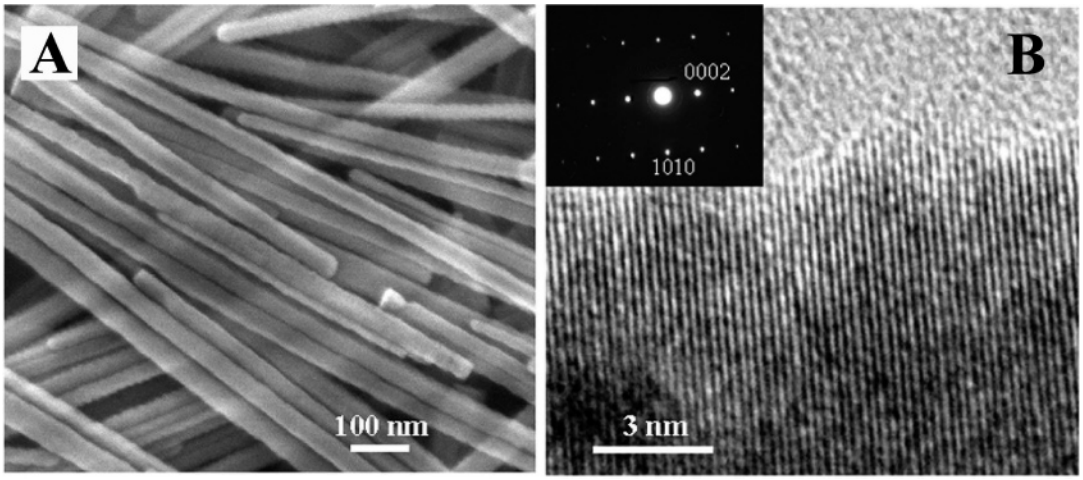

Figure 5. (A) SEM and (B) high-resolution TEM characterization of cobalt-doped ZnO nanowires. Cobalt content = 11.34 atom %. Reprinted with permission from ref 16. Copyright 2005 Wiley-VCH.

Controlled Doping of ZnO Nanowires. The primary method of controlling the properties of bulk semiconductors, such as electrical conductivity, is through the introduction of impurity atoms, or dopants. Doping in nanostructures is nontrivial because the dopants must disperse isotropically throughout the host semiconductor matrix without dopant overgrowth or phase separation. Dopants are usually incorporated into ZnO nanowires during wire growth. In vapor-phase syntheses, the dopant is carried into the reaction furnace along with the constituent precursors, while in solution-phase syntheses, it is codissolved at the start of the reaction.

Doping can be difficult in aqueous systems because the dopant species can easily form aquo ions and not be incorporated into the crystal lattice. This is particularly true for first-period transition metals, nearly all of which form stable, inert complexes with water. Recently, transition-metal doping of ZnO nanowires in aqueous solutions has been demonstrated by applying a reducing potential to the growth substrate that favors doping over metal−aquo complex formation.[48,49]

Doping in nonaqueous solvents avoids the formation of inert metal−aquo complexes and also enables a higher reaction temperature. Cobalt-doped ZnO nanowires have been synthesized by codissolving a desired amount of cobalt acetate, $Co(OAc)_2$, with zinc acetate in trioctylamine. Using this approach, large quantities of single-crystalline, transition-metal-doped ZnO nanowires are obtained with excellent purity, free from dopant overgrowth and secondary phases (Figure 5). Other transition metals that have been incorporated into the ZnO lattice using this method include manganese, iron, and copper.[16]

Magnetic Properties for DMSs

ZnO is expected to become a DMS when it is doped with a first-row transition metal. DMS materials, which also include other II−VI or III−V semiconductors (e.g., GaN, ZnS, GaAs) doped with transition metals, are currently the subject of intense research, principally for their potential use in spin-based electronic, or "spintronic", devices, where the spin of the electron is utilized in addition to its charge. A few prototypical spin-based light-emitting diodes (LEDs) have been fabricated;[50,51] these devices employ a series of DMS quantum dots embedded between the p- and n-type layers of the LED. The ferromagnetic behavior of the DMS causes the emitted light to be circularly polarized. Most ZnO DMS research is done on thin films[52−55] or quantum dots,[8,56] with very few reports on transition-metal-doped ZnO nanowires. Most of these studies employ high-temperature, vapor-phase synthetic methods,[57,58] and their results have been reviewed elsewhere.[59,60]

The structural and magnetic properties of cobalt-doped ZnO nanowires grown in trioctylamine have been studied,[16] with PL and XRD data showing that the added cobalt substitutes directly for zinc ions in the wurtzite lattice. Figure 6A shows XRD patterns from a series of nanowires with different cobalt concentrations (0−11 atom %). In all cases,

(47) Andelman, T.; Gong, Y. Y.; Polking, M.; Yin, M.; Kuskovsky, I.; Neumark, G.; O'Brien, S. *J. Phys. Chem. B* **2005**, *109*, 14314−14318.
(48) Cui, J. B.; Gibson, U. J. *Appl. Phys. Lett.* **2005**, 87.
(49) Cui, J. B.; Gibson, U. J. *J. Phys. Chem. B* **2005**, *109*, 22074−22077.
(50) Chakrabarti, S.; Holub, M. A.; Bhattacharya, P.; Mishima, T. D.; Santos, M. B.; Johnson, M. B.; Blom, D. A. *Nano Lett.* **2005**, *5*, 209−212.
(51) Kioseoglou, G.; Hanbicki, A. T.; Sullivan, J. M.; van't Erve, O. M. J.; Li, C. H.; Erwin, S. C.; Mallory, R.; Yasar, M.; Petrou, A.; Jonker, B. T. *Nat. Mater.* **2004**, *3*, 799−803.
(52) Buchholz, D. B.; Chang, R. P. H.; Song, J. H.; Ketterson, J. B. *Appl. Phys. Lett.* **2005**, 87.
(53) Jedrecy, N.; von Bardeleben, H. J.; Zheng, Y.; Cantin, J. L. *Phys. Rev. B* **2004**, *69*.
(54) Kundaliya, D. C.; Ogale, S. B.; Lofland, S. E.; Dhar, S.; Metting, C. J.; Shinde, S. R.; Ma, Z.; Varughese, B.; Ramanujachary, K. V.; Salamanca-Riba, L.; Venkatesan, T. *Nat. Mater.* **2004**, *3*, 709−714.
(55) Ramachandran, S.; Tiwari, A.; Narayan, J. *Appl. Phys. Lett.* **2004**, *84*, 5255−5257.
(56) Schwartz, D. A.; Norberg, N. S.; Nguyen, Q. P.; Parker, J. M.; Gamelin, D. R. *J. Am. Chem. Soc.* **2003**, *125*, 13205−13218.
(57) Chang, Y. Q.; Wang, D. B.; Luo, X. H.; Xu, X. Y.; Chen, X. H.; Li, L.; Chen, C. P.; Wang, R. M.; Xu, J.; Yu, D. P. *Appl. Phys. Lett.* **2003**, *83*, 4020−4022.
(58) Wu, J. J.; Liu, S. C.; Yang, M. H. *Appl. Phys. Lett.* **2004**, *85*, 1027−1029.
(59) Ohno, H. *J. Magn. Magn. Mater.* **1999**, *200*, 110−129.
(60) Prellier, W.; Fouchet, A.; Mercey, B. *J. Phys.: Condens. Matter* **2003**, *15*, R1583−R1601.

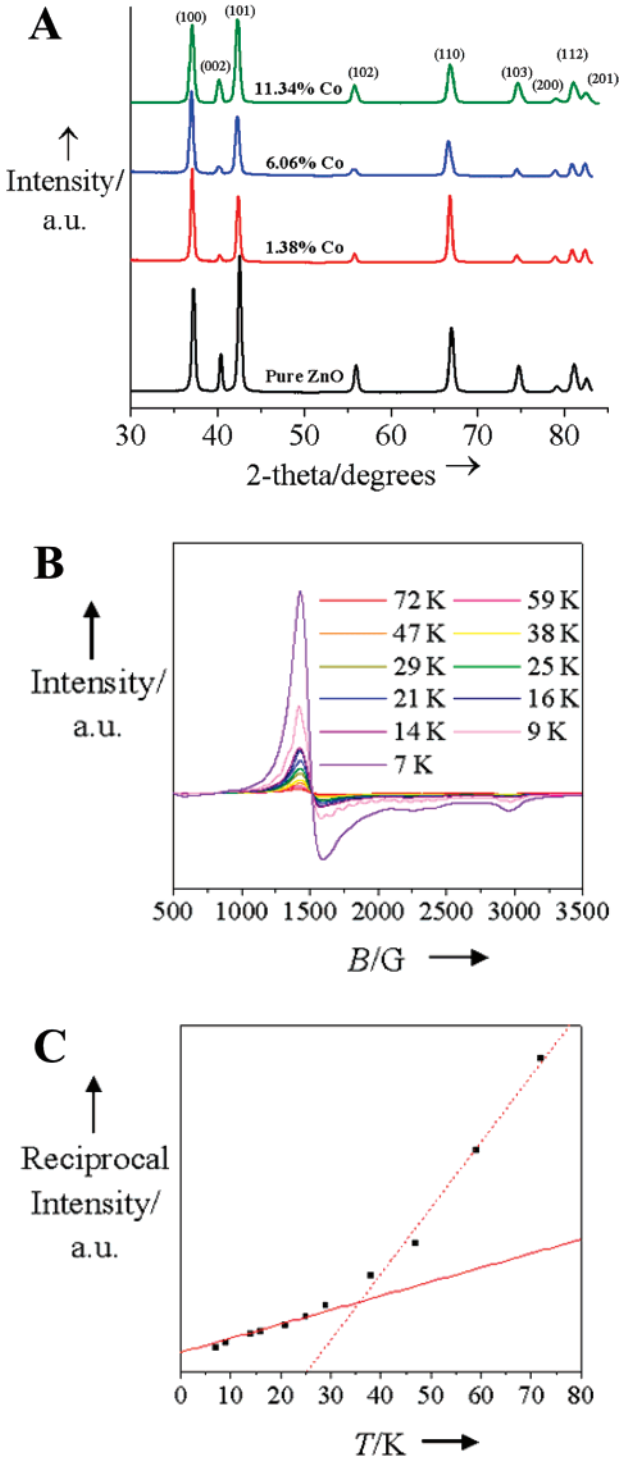

Figure 6. Analysis of cobalt-doped ZnO nanowires. (A) XRD of nanowires with various cobalt doping concentrations. (B) Temperature-dependent EPR spectra. Cobalt concentration = 2.15 atom %. (C) Reciprocal intensity versus temperature graph for the same sample as that used in B. Intensities were obtained by numerical integration of the as-collected spectra twice. The solid line is a plot of the Curie law, and the dashed line is fitted to the higher-temperature data points. Reprinted with permission from ref 16. Copyright 2005 Wiley-VCH.

wurtzite is the only phase present. Electron diffraction supports these data, showing that cobalt can be incorporated into a ZnO lattice without apparent phase segregation at a doping level greater than 11 atom %.

Figure 6B shows an EPR spectrum of $Zn_{1-x}Co_xO$ (x = 0.021) nanowires at various temperatures. In Figure 6C, the reciprocal intensity of the EPR signal is plotted versus temperature. A clear deviation from Curie law behavior is seen in the temperature range 25−30 K, with a similar deviation from paramagnetic behavior seen in SQUID magnetometry experiments. Although characterization of the cobalt-doped ZnO wires suggests uniform doping, we note the existence of complex magnetic behavior that raises the possibility of multiple magnetic phases. Transition-metal-doped ZnO is predicted to be ferromagnetic at room temperature,[61,62] but experimental observations on the magnetism vary widely, ranging from no magnetic ordering[63] to superparamagnetic behavior[64] to ferromagnetism above 500 K.[65] The conflicting reports suggest either that magnetism cannot be modeled by a simple ferromagnetic or paramagnetic mechanism or that sample quality is variable in these cases. This inconsistency is the subject of ongoing research.

Vertical Nanowire Arrays from Textured ZnO Seeds

Vertical ZnO nanowire arrays may be beneficial to the performance of certain devices, such as polymer−inorganic solar cells,[66] UV lasers,[3] and vertical-field-effect transistors.[67] Ordered arrays can be grown from a single-crystalline substrate that has a small lattice mismatch and appropriate symmetry (usually Al_2O_3 or GaN).[3,68] Alternatively, a ZnO thin film[22,69] or a discontinuous layer of nanoscopic ZnO seeds[17] deposited on a nonepitaxial substrate (such as silicon or glass) can act as a nucleation layer for wire growth. For device applications, vertical growth from textured ZnO seeds is appealing because the processing is low-cost, versatile, and substrate-independent. Also, the nanowires can have direct contact with the substrate without sitting atop a disordered polycrystalline film.

Recently, we produced textured ZnO seeds by thermally decomposing a thin layer of zinc acetate on a substrate.[17] First, a substrate is wetted with a droplet of 0.005 M zinc acetate dihydrate in ethanol, rinsed with ethanol after 10 s, and then blown dry. This step is repeated three to five times to ensure a complete coverage of seeds. Upon heating above 200 °C, the zinc acetate crystallites decompose to form ZnO islands, with their (0001) planes parallel to the substrate surface. The alignment is substrate-independent and occurs on any flat surface regardless of the surface crystallinity and chemistry. Vertical wires have been grown on ZnO and Al_2O_3

(61) Dietl, T.; Ohno, H.; Matsukura, F.; Cibert, J.; Ferrand, D. *Science* **2000**, *287*, 1019−1022.
(62) Sato, K.; Katayama-Yoshida, H. *Phys. E (Amsterdam, Neth.)* **2001**, *10*, 251−255.
(63) Lawes, G.; Risbud, A. S.; Ramirez, A. P.; Seshadri, R. *Phys. Rev. B* **2005**, 71.
(64) Park, J. H.; Kim, M. G.; Jang, H. M.; Ryu, S.; Kim, Y. M. *Appl. Phys. Lett.* **2004**, *84*, 1338−1340.
(65) Deka, S.; Pasricha, R.; Joy, P. A. *Chem. Mater.* **2004**, *16*, 1168−1169.
(66) Kannan, B.; Castelino, K.; Majumdar, A. *Nano Lett.* **2003**, *3*, 1729−1733.
(67) Ng, H. T.; Han, J.; Yamada, T.; Nguyen, P.; Chen, Y. P.; Meyyappan, M. *Nano Lett.* **2004**, *4*, 1247−1252.
(68) Park, W. I.; Kim, D. H.; Jung, S. W.; Yi, G. C. *Appl. Phys. Lett.* **2002**, *80*, 4232−4234.
(69) Henley, S. J.; Ashfold, M. N. R.; Nicholls, D. P.; Wheatley, P.; Cherns, D. *Appl. Phys. A: Mater. Sci. Process.* **2004**, *79*, 1169−1173.

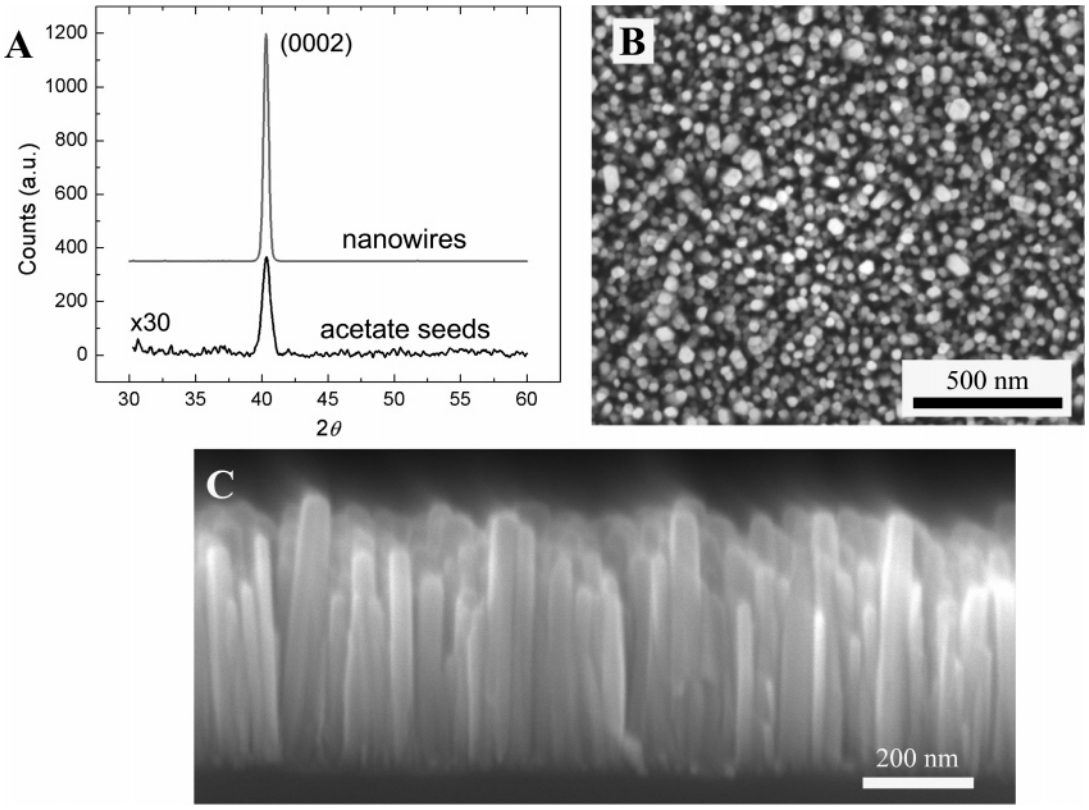

Figure 7. Vertical alignment of ZnO nanowire arrays using textured seeds. (A) XRD and (B) plan view SEM data for an array grown from ZnO nanocrystal seeds that were formed in situ on a silicon surface from the decomposition of zinc acetate at 350 °C. (C) Cross-sectional SEM image of an array showing the absence of an intermediate nanoparticle layer.

single crystals, transparent conducting oxides, amorphous oxides including glass and silicon with its native oxide, and metals such as gold and titanium. XRD of the seeds prior to growth shows only a (0002) reflection, evidence of the *c*-axis texturing. The resulting array, grown using zinc nitrate and HMTA synthesis in water, has the same orientation as the ZnO seeds (Figure 7A). An SEM cross-sectional image of the array shows no intermediate thin film of ZnO. This technique has been expanded to ZnO nanowire growth in the gas phase[17] and might also be useful in nonaqueous solvents.

ZnO Nanowire DSCs

The DSC is promising as a potentially inexpensive alternative to conventional silicon-based solar cells. Crucial to its performance is a thick nanoparticle film that provides a large surface area for the adsorption of light-harvesting dye molecules. This nanoparticle photoanode is usually constructed with 10-μm-thick films of TiO_2 or, sometimes, ZnO or SnO_2.[70−73] During operation, the dye molecules are excited by light and create excitons that are rapidly split at the nanoparticle interface, injecting electrons into the film. The electrons travel through the nanoparticle film by way of trap-limited diffusion, a slow mechanism that can limit the device efficiency. A promising approach for improving the efficiency of the DSC is to replace the nanoparticle film with an array of oriented single-crystalline nanowires (Figure 8A). Electron transport through these wires is expected to be several orders of magnitude faster than that by the random-walk mechanism associated with a nanoparticle film. This may increase the electron diffusion length in the device and allow for thicker cells with greater dye loading and the use of solid-state electrolytes.

We replaced the nanoparticle film with a dense, oriented array of crystalline ZnO nanowires grown using zinc nitrate, HMTA, and PEI in water. Using a ZnO nanowire array with one-fifth the surface area of a nanoparticle DSC, a full sun efficiency of 1.5% was demonstrated.[7] Figure 8B is a plot of the current density versus voltage ($J-V$) for our two best devices with roughness factors (defined as the total film area per unit substrate area) of ∼200. Nanoparticle films typically have a roughness factor of ∼1000. The external quantum efficiency (EQE) of these cells peaks at ∼40% near the absorption maximum of the dye molecule {[*cis*-bis(thiocyanato)-*N*,*N*′-bis(2,2″-bipyridyl-4,4′-dicarboxylate)ruthenium-(II) bis(tetrabutylammonium)], also known as N719}. The EQE is mainly limited by the low dye loading of the nanowire films because of a relatively small roughness factor.

To understand the relative electron transport of the nanowire cell versus the nanoparticle cell, it is best to compare the short-circuit current density (J_{SC}) rather than

(70) Keis, K.; Magnusson, E.; Lindstrom, H.; Lindquist, S. E.; Hagfeldt, A. *Sol. Energy Mater. Sol. Cells* **2002**, *73*, 51−58.
(71) Nazeeruddin, M. K.; Pechy, P.; Renouard, T.; Zakeeruddin, S. M.; Humphry-Baker, R.; Comte, P.; Liska, P.; Cevey, L.; Costa, E.; Shklover, V.; Spiccia, L.; Deacon, G. B.; Bignozzi, C. A.; Gratzel, M. *J. Am. Chem. Soc.* **2001**, *123*, 1613−1624.
(72) Rensmo, H.; Keis, K.; Lindstrom, H.; Sodergren, S.; Solbrand, A.; Hagfeldt, A.; Lindquist, S. E.; Wang, L. N.; Muhammed, M. *J. Phys. Chem. B* **1997**, *101*, 2598−2601.
(73) Tennakone, K.; Kumara, G.; Kottegoda, I. R. M.; Perera, V. P. S. *Chem. Commun.* **1999**, 15−16.

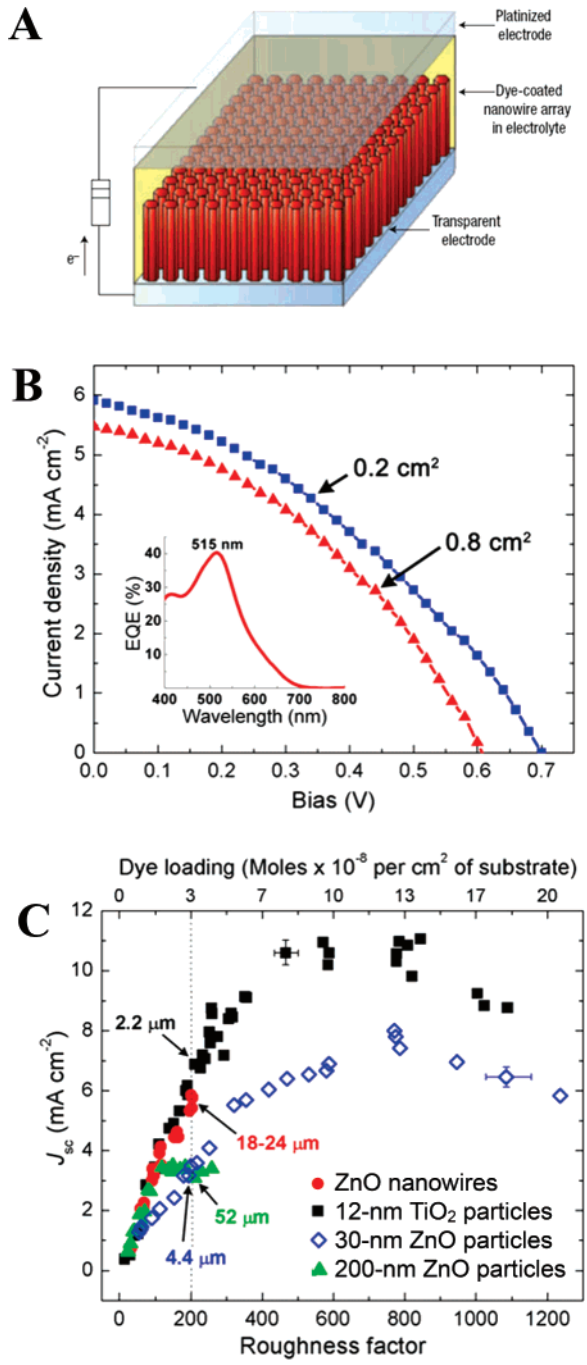

Figure 8. Nanowire dye-sensitized cell, based on a ZnO nanowire array. (A) Schematic diagram of the cell. Light is incident through the bottom electrode. (B) Device performance under AM 1.5G illumination for two cells with roughness factors of ~200. Traces of the current density versus voltage ($J-V$) for a small cell (active area, 0.2 cm^2; efficiency of 1.51%) and a large cell (0.8 cm^2; 1.26%). Inset: EQE versus wavelength for the large cell. (C) Comparative performance of nanowire and nanoparticle cells. Short-circuit current density (J_{SC}) versus roughness factor for cells based on ZnO nanowires, 12-nm TiO_2 particles, and 30- and 200-nm ZnO particles. Error bars are an estimate of the maximum range of the values and are limited to maximize figure clarity. Cell size: 0.8 cm^2. Reprinted with permission from ref 7. Copyright 2005 Nature.

the absolute efficiency. This is because J_{SC} is the amount of current extracted from the device at short-circuit conditions and is proportional to the efficiency at which the current is collected, while for a given light intensity, the overall cell efficiency is dependent on three parameters [J_{SC}, open-circuit voltage (V_{OC}), and fill factor]. Figure 8C plots J_{SC} versus roughness factor for nanoparticle cells (12-nm TiO_2 particles and 30- and 200-nm ZnO particles) and nanowire cells. The nanowire cells show a nearly linear increase in J_{SC} with an increase in the roughness factor. The data almost lie directly on the TiO_2 nanoparticle data, which is significant because transport is very efficient in thin TiO_2 nanoparticle films. This shows strong evidence for an equally high collection efficiency for nanowire cells with wires as long as 25 μm. Furthermore, the ZnO nanowire cells generate considerably higher currents than either of the ZnO nanoparticle cells, suggesting the superiority of the nanowire photoanode as a charge collector. This nanowire architecture may also show an improvement in the charge collection for polymer−inorganic solar cells. These devices are currently being tested in our laboratory.

Conclusion

We review several strategies for growing ZnO nanowires in solution with emphasis on the hydrolysis of zinc nitrate with HMTA and the decomposition of zinc acetate in trioctylamine. Wires grown via the aqueous route have diameters <100 nm when grown from a seeded substrate. When PEI is added, the lengths of the wires can exceed 20 μm with aspect ratios above 125. The aqueous solution synthesis provides a ready means to tune the wire diameter, length, and aspect ratio.

The decomposition of zinc acetate in trioctylamine forms nanowire bundles that are typically 0.5−6 μm in length and 25−35 nm in diameter. This nonaqueous route offers a simple approach to fabricating doped ZnO, particularly transition-metal-doped nanowires. In particular, cobalt-doped ZnO nanowires are uniformly doped, with magnetic studies showing a clear deviation from paramagnetic behavior between 25 and 30 K.

Decomposing zinc acetate crystallites on a substrate forms ZnO islands, with their (0001) planes parallel to the substrate surface. The use of a flat substrate with textured seeds that act as nucleation sites for ZnO nanowire growth produces vertical wire arrays. A full sun efficiency of 1.5% was demonstrated with a nanowire photoanode having one-fifth the surface area of a nanoparticle DSC. Comparative studies between nanoparticle and nanowire cells show that the direct electrical pathway provided by the nanowires allows the current to be collected more efficiently from the device. Solution-phase one-dimensional ZnO syntheses may have an important role to play in emerging applications. The ease of synthesis, ability to control orientation, dimensionality, dopants, and doping concentrations make this approach very promising.

Acknowledgment. This work is supported by National Science Foundation and Office of Basic Science, Department of Energy. P.Y. is a Dreyfus Teacher−Scholar. We thank Rongrui He and Dr. Donald Sirbuly for TEM and optical measurements. We thank the National Center for Electron Microscopy for the use of their facilities.

IC0601900